



Discover Generics

Cost-Effective CT & MRI Contrast Agents



FRESENIUS
KABI

WATCH VIDEO

AJNR

Water Diffusion Compartmentation at High b Values in Ischemic Human Brain

Pierre Brugières, Philippe Thomas, Anne Maraval, Hassan Hosseini, Catherine Combes, Abdallah Chafiq, Lucile Ruel, Stéphane Breil, Marc Peschanski and André Gaston

This information is current as of June 9, 2025.

AJNR Am J Neuroradiol 2004, 25 (5) 692-698
<http://www.ajnr.org/content/25/5/692>

Water Diffusion Compartmentation at High b Values in Ischemic Human Brain

Pierre Brugières, Philippe Thomas, Anne Maraval, Hassan Hosseini, Catherine Combes, Abdallah Chafiq, Lucile Ruel, Stéphane Breil, Marc Peschanski, and André Gaston

BACKGROUND AND PURPOSE: We studied the evolution of brain water compartments during the early stage of ischemic stroke.

METHODS: Diffusion-weighted imaging was performed at 1.5 T in 10 volunteers and 14 patients with stroke. We used a single-shot echo-planar technique with 11 b values of 0–5000 s/mm². Regions of interest were selected in the white matter (WM) and striatum of the volunteers and in the ischemic core of the patients. Measurements were fitted on the basis of a biexponential decay with the b factor as follows: $S(b) = S(0)[(f_{\text{slow}} \times \exp(-b \times \text{ADC}_{\text{slow}}) + (f_{\text{fast}} \times \exp(-b \times \text{ADC}_{\text{fast}}))]$ where $S(b)$ is the signal intensity in the presence of a diffusion gradient, $S(0)$ is the signal intensity without diffusion sensitization, ADC_{slow} and ADC_{fast} are the respective apparent diffusion coefficients (ADCs) of slow diffusing compartments (SDCs) and fast diffusing compartments (FDCs), and f_{slow} and f_{fast} the respective contributions to the signal intensity of SDC and FDC.

RESULTS: In healthy subjects, FDC represents $74.3 \pm 3.1\%$ of brain water, with $\text{ADC}_{\text{fast}} = (124.6 \pm 12.0) \times 10^{-5} \text{ mm}^2/\text{s}$ and $\text{ADC}_{\text{slow}} = (15.5 \pm 3.9) \times 10^{-5} \text{ mm}^2/\text{s}$. In stroke, decreased FDC ($49.1\% \pm 10.9\%$; $P = 1.05 \times 10^{-5}$) and increased ADC_{slow} ($[22.4 \pm 8.1] \times 10^{-5} \text{ mm}^2/\text{s}$; $P = 8.07 \times 10^{-3}$) were observed, but ADC_{fast} was not significantly changed ($[135.6 \pm 25.7] \times 10^{-5} \text{ mm}^2/\text{s}$; $P = .151$).

CONCLUSION: The restricted diffusion observed in the early stroke is mainly related to a redistribution of water from the FDC to the SDC.

Diffusion-weighted MR imaging (DWI) is a sensitive technique for measuring random microscopic motion of brain water (1) and routinely used for the early diagnosis of stroke (2–5). At the acute stage of ischemic stroke, cell swelling (a consequence of failure of the adenosine triphosphate-dependent ionic pump) is generally thought to reduce the apparent diffusion coefficient (ADC) of brain water. Nevertheless, the compartmentation of the restricted water is still controversial. Theoretic evidence indicates that the ADC of water in brain ischemia may be related to the variation of the volume fraction of the interstitial space. The redistribution of water from the extracellular to the intracellular space is then believed to be responsible for the change in ADC observed in ischemic brain tissue (6).

In clinical practice, two or three measurements of signal intensity with different b values (usually lower than 1000 s/mm²) are performed for ADC extraction. Clinical ADC measurement is then founded on the hypothesis of a monoexponential signal intensity decay with a b factor. Some have reported that the signal intensity of brain water shows a non-monoexponential decay when measured over a b factor range of up to 5000 s/mm². Two separate water compartments with different diffusion coefficients (thought to be related to extracellular water, at least for the compartment with higher ADC) may be inferred on the basis of a biexponential model fitted for water signal intensity decay with the b factor (7–12).

The purpose of this study was to investigate the evolution of brain water compartments during the course of ischemic stroke.

Methods

Fourteen stroke patients with restricted diffusion on conventional DWI had DWI study with high b factors. All were admitted to our institution in the first 7 days after the onset of a neurologic deficit. All studies were performed within the guidelines of our institutional internal review board, and informed consent was obtained from the patients and healthy subjects.

Received March 27, 2003; accepted after revision October 10.

From the Departments of Neuroradiology and Neurology (P.B., P.T., A.M., C.C., A.C., A.G.), Henri Mondor Hospital, Neurology (H.H.), Créteil; Siemens SA, St Denis; and INSERM U421 (P.B., H.H., M.P.), Créteil, France.

Address reprint requests to Pierre Brugières, Henri Mondor Hospital, Neuroradiology, 51 ave du Mal de Lattre de Tassigny, Créteil 94000, France.

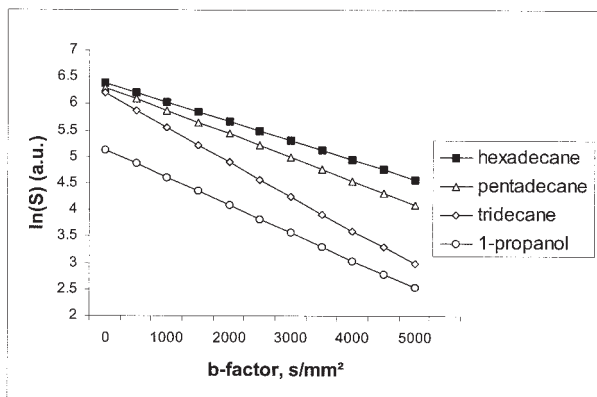


FIG 1. Diffusion attenuation in test liquids at 22°C indicates a monoexponential signal intensity decay with the b factor.

DWI was performed on a whole-body 1.5-T imager (Symphony Quantum; Siemens, Erlangen, Germany) with a gradient strength of 30 mT/m, a slew rate of 125 T/m/s, and use of a head coil. We used a single-shot echo-planar technique (TR/TE/NEX = 1000/123/10, FOV = 250×250 mm, matrix = 128×128 , section thickness = 5 mm) with 11 b values of 0, 500, 1000, 1500, 2000, 2500, 3000, 3500, 4000, 4500, and 5000 s/mm². This was based on the method of Stejskal and Tanner described (13). Diffusion encoding was performed along the x , y , and z axes to obtain the trace of the diffusion tensor.

Regions of interest (ROIs) were selected in the frontal white matter (WM) and the striatum of 10 healthy volunteers. In the patient group, ROIs were selected 1) in the hyperintense area on DWI and the area with restricted diffusion on the clinical ADC map (This was calculated on the basis of a monoexponential decrease of the signal intensity with b , with b factors of 0, 500, and 1000 mm²/s.) and 2) in the symmetrical, contralateral, normal brain.

Signal intensity in the ROIs was measured for each b factor. We used Mathcad software developed in-house to fit the measurements based on a biexponential decay with the b factor, as follows: $S(b) = S(0)[f_{\text{slow}} \times \exp(-b \times \text{ADC}_{\text{slow}}) + (f_{\text{fast}} \times \exp(-b \times \text{ADC}_{\text{fast}}))]$ where $S(b)$ is the signal intensity in the presence of a diffusion gradient, $S(0)$ is the signal intensity without diffusion sensitization, ADC_{slow} and ADC_{fast} are the respective apparent diffusion coefficients (ADCs) of slow diffusing compartments (SDCs) and fast diffusing compartments (FDCs), and f_{slow} and f_{fast} the respective contributions to the signal intensity of SDC and FDC.

We assessed the respective ADCs values and the contribution to the signal intensity of the SDCs and the FDCs in both patients and volunteers. Maps of the fitted parameters (f_{fast} , ADC_{fast} , ADC_{slow}) were calculated on a Mathcad software developed at our institution. To verify that instrumental factors were not responsible for the biexponential pattern of the signal-intensity decay, measurements were made at room temperature (22°C), with the same imaging techniques. For this, we used phantoms filled with n -alkanes (tridecane, pentadecane, and hexadecane) and 1-propanol.

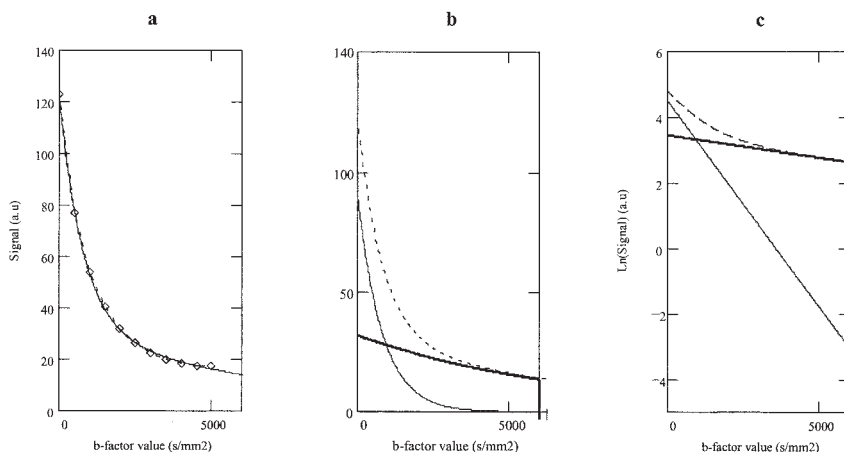


FIG 2. Biexponential decay curves for ROIs in the WM in healthy volunteer 8. *Left*, Curve fits the measured points (diamonds). *Middle and right*, The signal intensity (dotted line) originates from two compartments: an FDC (thin solid line) and an SDC (thick bold line). f_{fast} represents 74.1% of the total brain water. ADC_{fast} and ADC_{slow} values are 125.7×10^{-5} and 13.6×10^{-5} mm²/s, respectively. In C, the semi-log representation of the evolution of signal intensity with b factor shows an obvious biexponential decay.

TABLE 1: Fast and slow ADCs and fast-diffusion fraction of brain water in healthy volunteers

Volunteer	Frontal WM			Basal Ganglia		
	f_{fast} (%)	ADC_{fast} ($\times 10^{-5}$ mm ² /s)	ADC_{slow} ($\times 10^{-5}$ mm ² /s)	f_{fast} (%)	ADC_{fast} ($\times 10^{-5}$ mm ² /s)	ADC_{slow} ($\times 10^{-5}$ mm ² /s)
1	72.1	123.7	7.5	75.9	147.7	10.8
2	77.1	130.1	12.2	76.5	96.0	18.6
3	75.8	135.7	10.7	73.0	125.6	13.1
4	71.1	142.9	21.3	78.0	116.9	16.2
5	71.9	127.8	15.0	81.6	99.0	24.7
6	79	122.1	18.6	71.1	123.5	16.4
7	72.8	128	16	71.8	120.1	13.4
8	74.1	125.7	13.6	70.9	133.5	18.5
9	74.6	122.5	13.6	71.9	127.8	15.0
10	75.3	122.5	16.0	70.8	120.1	18.4
Mean	74.4	128.1	14.4	74.2	121.0	16.5
SD	2.5	6.7	3.9	3.7	15.2	3.9

TABLE 2: Clinical ADC values

Patient	Days from Ictus	Location	ROI (cm ²)	Infarcted Tissue				Normal Contralateral Brain			
				f_{fast} (%)	ADC _{fast} ($\times 10^{-5}$ mm ² /s)	ADC _{slow} ($\times 10^{-5}$ mm ² /s)	ADC, $b = 1000$ s/mm ² ($\times 10^{-5}$ mm ² /s)	f_{fast} (%)	ADC _{fast} ($\times 10^{-5}$ mm ² /s)	ADC _{slow} ($\times 10^{-5}$ mm ² /s)	ADC, $b = 1000$ s/mm ² ($\times 10^{-5}$ mm ² /s)
1	3	R MCA	2.53	48.3	123.9	17.5	54.8	72.3	130.3	14.4	81.7
2	3	R PICA	0.53	51.1	102.0	15.0	50.0	76.2	110.0	12.0	75.0
3	1	L MCA	0.38	42.8	109.2	22.2	51.3	75.4	112.1	19.4	79.6
4	2	R ALA	0.32	28.3	132.9	31.8	53.5	74.9	136.6	10.7	87.0
5	3	R MCA	0.92	45.3	197.4	36.3	78.4	70.1	145.3	28.7	94.0
6	7	L MCA	14.2	49.9	116.8	10.2	49.6	69.5	119.3	12.6	73.5
7	1	L MCA	3.07	54.4	163.6	17.1	69.7	73.7	124.1	12.7	80.3
8	1	L MCA	7.95	57.3	133.0	22.0	71.0	74.8	117.6	9.9	77.1
9	3	R MCA	2.85	29.8	142.0	33.0	57.0	70.9	133.0	19.0	86.0
10	6	L MCA	0.45	63.6	132.0	14.0	72.0	70.8	137.0	20.0	86.0
11	7	L PICA	0.42	58.1	145.0	23.0	75.0	62.5	149.0	23.0	82.0
12	6	L MCA	3.07	65.9	113.0	17.0	69.0	70.4	131.0	15.0	80.0
13	7	R MCA	0.48	48.8	123.0	22.0	59.0	80.2	110.0	8.0	81.0
14	1	R ACA	0.21	44.3	165.0	33.0	72.0	73.0	115.0	14.0	77.0
Mean	NA	NA	NA	49.1	135.6	22.4	63.0	72.5	126.5	15.7	81.4
SD	NA	NA	NA	10.9	25.7	8.1	10.3	4.1	12.9	5.7	5.4

Note.—ADCs were calculated with b factors of 0, 500, and 1000 mm²/s; ADC_{fast} and ADC_{slow}; ACA indicates anterior cerebral artery; MCA, middle cerebral artery; NA, not applicable; PICA, posterior-inferior cerebellar artery.

Measurements obtained in the ischemic tissue and in the contralateral normal brain of the patients were analyzed by using a Student paired t test. P values less than .05 indicated a significant difference.

Results

The signal-intensity decay as a function of b factor was found to be monoexponential for all test liquids (Fig 1). Measured diffusion coefficients were 0.653×10^{-3} mm²/s for tridecane, 0.439×10^{-3} mm²/s for pentadecane, 0.362×10^{-3} mm²/s for hexadecane, and 0.569×10^{-3} mm²/s for 1-propanol.

The signal intensity decay as a function of b factor was in close agreement with results from a biexponential model in the volunteers. Figure 2 shows the measurements obtained in the normal frontal WM of a healthy subject with b factors of 0–5000 s/mm² and the biexponential fit of the data points. Brain water appeared to be mainly represented by the FDC in the volunteers ($f_{\text{fast}} = 74.3\% \pm 3.1\%$), with a mean ADC_{fast} of $(124.6 \pm 12.0) \times 10^{-5}$ mm²/s and a mean ADC_{slow} of $(15.5 \pm 3.9) \times 10^{-5}$ mm²/s. Table 1 shows the respective values of ADC_{slow}, ADC_{fast}, and f_{fast} in the gray matter (GM) and WM of the healthy volunteers.

Table 2 shows the ADC_{fast}, ADC_{slow}, and f_{fast} values calculated in the 14 patients at the level of the infarct and in the contralateral normal-appearing WM. The patients had a mean clinical ADC value of $(63.0 \pm 10.3) \times 10^{-5}$ mm²/s and a mean f_{fast} values of $49.1\% \pm 10.9\%$ at the level of the infarcted tissue. In the ischemic parenchyma we found a mean ADC_{fast} of $(135.6 \pm 25.7) \times 10^{-5}$ mm²/s and a mean ADC_{slow} of $(22.4 \pm 8.1) \times 10^{-5}$ mm²/s. In the normal-appearing WM of the patients, f_{fast} was $72.5\% \pm 4.1\%$, ADC_{fast} was $(126.5 \pm 12.9) \times 10^{-5}$ mm²/s, ADC_{slow} was $(15.7 \pm 5.7) \times 10^{-5}$ mm²/s, and the clinical ADC was $(81.4 \pm 5.4) \times 10^{-5}$ mm²/s. Figure 3 shows the measurements and the fitted data collected in a patient on day 2, and Figure 4 shows the parametric maps calculated in a patient at day 3 after symptom onset.

Patients 1 and 8, respectively, underwent sequential studies on day 3 and 21 and on days 1, 3, and 5 after symptom onset (Figs 5 and 6).

Discussion

Our measurements in test liquids were in close agreement with values obtained by Tofts et al (14). Several reports have noted that biexponential fitting improves the representation of diffusion-related signal-intensity loss in the brain (7–11, 15). f_{fast} , ADC_{fast} and ADC_{slow} values in the volunteer group were globally in good agreement with those previously reported in rats (8) or and in human brain (10, 11).

The measured fractions of the two water compartments differed from those expected for the intracellular and extracellular water fractions (8, 16). It is therefore hazardous to consider the slow ADC component as intracellular water and the fast ADC component as extracellular water. Neverthe-

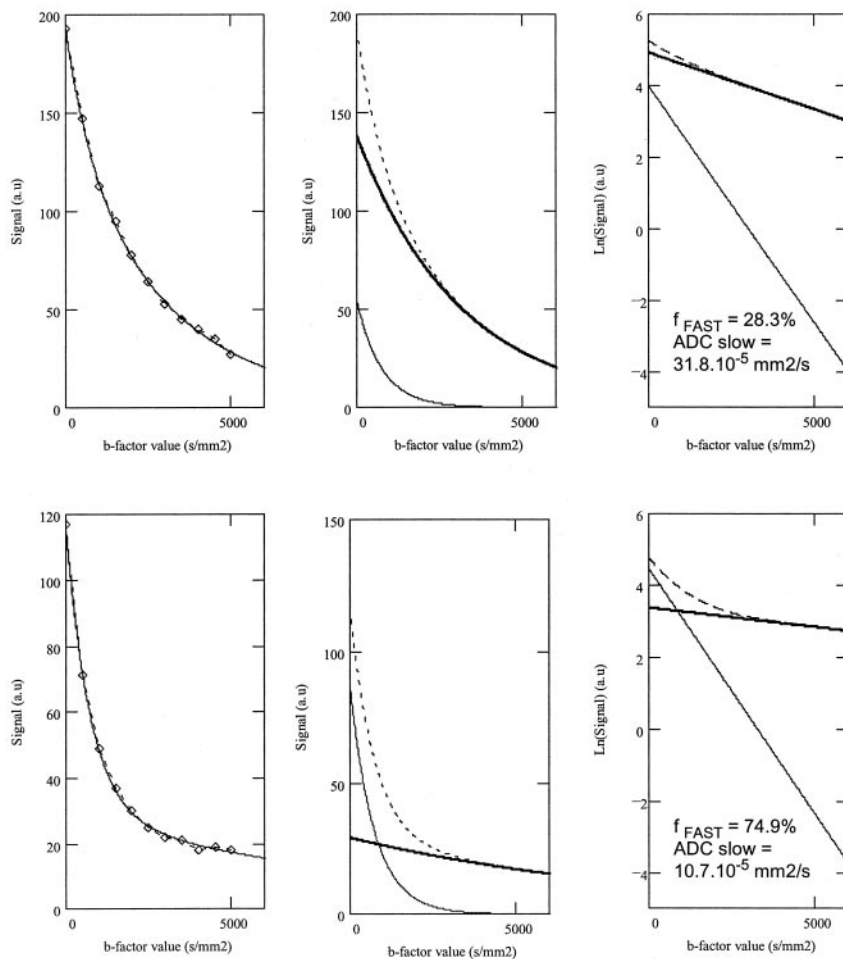


FIG 3. Biexponential decay of signal intensity measured in infarcted tissue (top row) and in normal contralateral WM (bottom row) in patient 4. The signal intensity (dotted line) originates from two compartments: an FDC (thin solid line) and an SDC (thick bold line). A dramatic decrease in f_{fast} associated with increased ADC_{slow} is observed in the infarcted tissue.

less, two findings—the magnitude of ADC_{fast} and measurements of tetramethyl ammonium diffusion in rat brain—are in agreement with the assignment of the fast-diffusing fraction of brain water to the extracellular space (11). Another point to consider is that the signal intensity measured on MR images (and then DWIs) is not a good representation of the total brain water but more obviously a representation of the brain water weakly linked to the pool of macromolecules.

Unlike previous observations (11, 15), we found no significant difference in the volunteer group between GM and WM values of f_{fast} (74.2% vs 74.4%; $P = .896$), ADC_{fast} (121.0×10^{-5} vs $128.1 \times 10^{-5} \text{ mm}^2/\text{s}$; $P = .252$), and ADC_{slow} (16.5×10^{-5} vs $14.4 \times 10^{-5} \text{ mm}^2/\text{s}$; $P = .177$). On the basis of 156 measurements in four volunteers, Clark and Le Bihan (11) found a small increase in ADC_{slow} (19×10^{-5} vs $16 \times 10^{-5} \text{ mm}^2/\text{s}$), a small decrease in ADC_{fast} (102×10^{-5} vs $112 \times 10^{-5} \text{ mm}^2/\text{s}$), and a small increase in f_{fast} (70% vs 66%) in GM versus WM. Maier et al (15) reported findings in 15 healthy subjects, noting a significant increase in both ADC_{slow} and ADC_{fast} in GM compared with WM. The small populations in the few available studies may account for the discrepancy in measurements. We found no significant difference between the GM and WM measurements of volun-

teers and the measurements in the normal parenchyma of the patients.

Diffusion imaging with high b values has been proposed for the evaluation of several pathologic conditions. Maier et al (15) used the technique to differentiate edema, tumor, normal GM, and normal WM. In stroke imaging, DWI with high b values may improve the conspicuity of small infarcts (17).

In our patients, measurements at the level of the ischemic core showed a biexponential decay of signal intensity with the b factor, a significant ($P = 1.05 \times 10^{-5}$) reduction in the fraction of the FDC (49.1% vs 72.5%), and a significant increase ($P = 8.07 \times 10^{-3}$) in ADC_{slow} (22.4×10^{-5} vs $15.7 \times 10^{-5} \text{ mm}^2/\text{s}$). We observed a slight but nonsignificant ($P = .197$) increase in ADC_{fast} (145.1×10^{-5} versus $126.5 \times 10^{-5} \text{ mm}^2/\text{s}$). Our results differ from those of Maier et al (15), who presented a single case with both decreased ADC_{slow} and decreased ADC_{fast} . However, they do not precisely describe the time delay between the occurrence of symptoms and the time of MR examination.

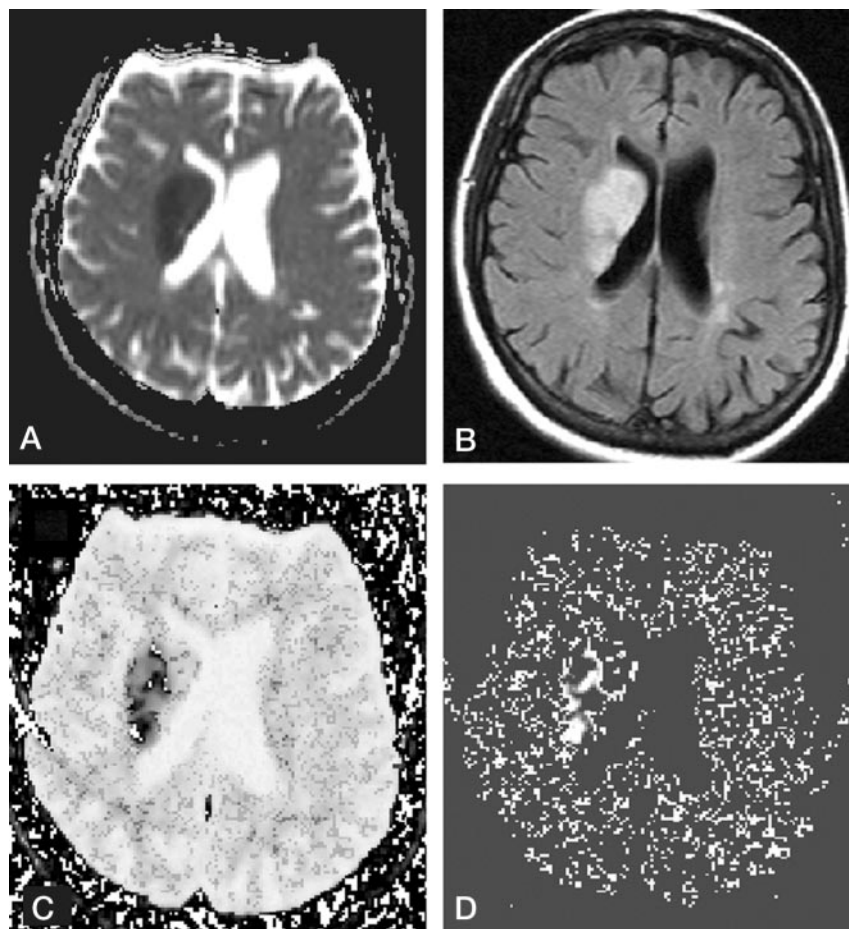
In the acute stage of ischemic stroke, decreased signal intensity on ADC maps during clinical DWI is thought to be related to the restricted motion of water at the level of the ischemic parenchyma. Our study demonstrates ADC at the level of the ischemic core is

FIG 4. Deep middle cerebral artery infarct at 72 hours after the onset of neurologic deficit in patient 9.

A and B, The infarcted parenchyma is hypointense on the global ADC map (A) and hyperintense on the fluid-attenuated inversion recovery image (B).

C, f_{fast} parametric map shows hypointensity at the level of the infarct.

D, ADC_{slow} parametric map shows increased ADC_{slow} in the infarcted tissue.



not reduced during the acute stage of stroke. On the contrary, we observed an increase of ADC_{slow} . If the SDC really corresponds to the intracellular compartment, the major increase in ADC_{slow} in our patients was probably related to cell swelling, the so-called cytotoxic edema observed in the first hours after an ischemic stroke if the adenosine triphosphate level decreases considerably. ADC_{fast} was obviously increased in three patients (patients 5, 7, and 14). This could have been due to early interstitial edema secondary to the breakdown of the blood-brain barrier. Unchanged ADC_{fast} and increased ADC_{slow} are unlikely to account for the apparent decrease in ADC on DWI in the acute stage of ischemic stroke.

The decreased signal intensity observed on clinical ADC maps was probably the consequence of the massive transfer of brain water from the FDC to the SDC. We observed a 33.2% decrease in the fraction of the FDC. The massive transfer of water from the FDC (thought to be extracellular) to the SDC (thought to be intracellular) may explain the decreased signal intensity of ischemic tissue on ADC maps, even if it was associated with increased ADC_{fast} and ADC_{slow} . The effect of f_{fast} on calculated clinical ADCs is presented in Table 3.

We were able to collect data during the evolution of brain infarction in two patients. ADC_{slow} progressively normalized, and ADC_{fast} increased in the isch-

emic tissue (Figs 5 and 6). This finding was in agreement with the regression of the cytotoxic edema and the occurrence of an extracellular edema.

Our data differ from the observations of Duong et al (18). Using 2-[^{19}F]fluoro-2-deoxyglucose-6-phosphate (2-FDG-6P), which they considered a valuable marker of the intracellular and extracellular spaces, Duong et al found no difference between intracellular and extracellular ADCs in normal or ischemic brain. They found a 40% ADC decrease in both compartments in ischemic rat brain; this was observed within 30 minutes after death and suggests that the loss of cytoplasmic circulation likely plays a major role in the decrease of intracellular ADC. However, whether 2-FDG-6P is a useful marker of water motion is unclear because, unlike water molecules, it does not pass through the plasma membranes. Using b factors of up to 6000 s/mm², Duong et al reported a mono-exponential decay of signal intensity for both intracellular and extracellular 2-FDG-6P.

In conclusion, our results show that the restricted diffusion demonstrated on clinical DWIs during early ischemic stroke is not related to decreased ADC in the SDC or FDC. Decreased signal intensity on ADC maps is explained only by a decrease in the fraction of the FDC related to the massive redistribution of the brain water from the FDC (thought to be extracellular) to the SDC. Our results provide additional evi-

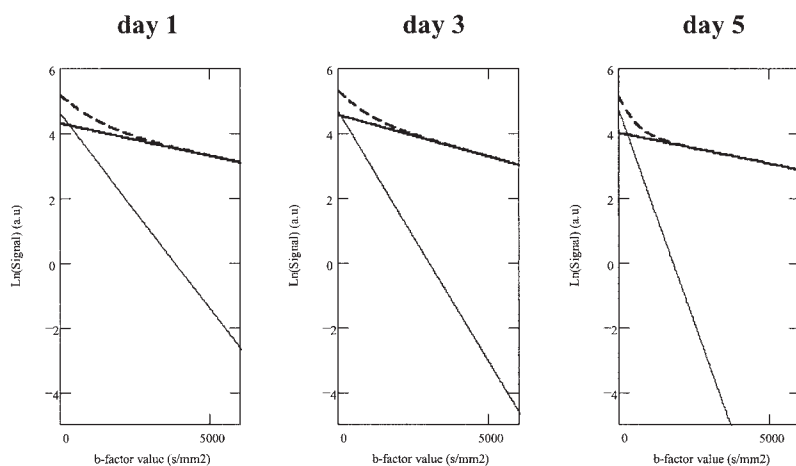


FIG 5. Temporal evolution of f_{fast} , ADC_{slow} ($\times 10^{-3} \text{ mm}^2/\text{s}$), and ADC_{fast} ($\times 10^{-3} \text{ mm}^2/\text{s}$) in patient 8 with ischemic stroke. The maximum decrease in f_{fast} and the maximum increase in ADC_{slow} are observed on day 3. An initial increase in both ADC_{slow} and ADC_{fast} is observed on days 1 and 3. On day 5, an increase in f_{fast} is associated with an increase in ADC_{fast} . This could have been the consequence of rupture of the blood-brain barrier.

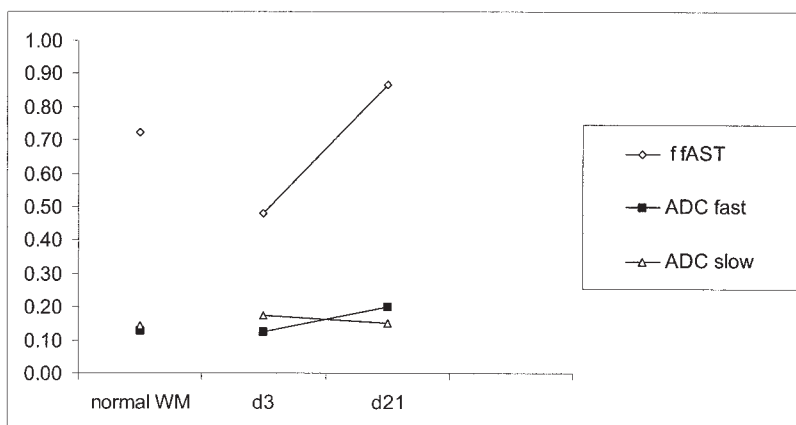
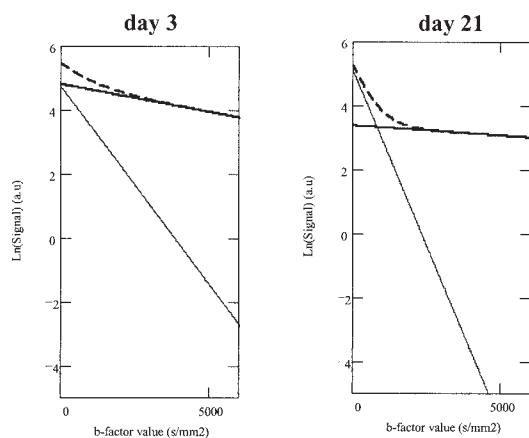
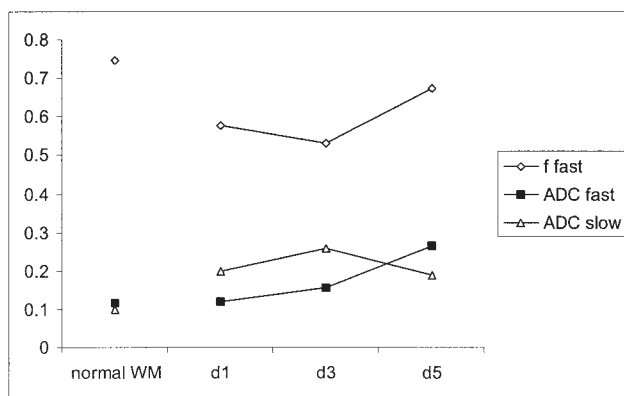


FIG 6. Temporal evolution of f_{fast} , ADC_{slow} ($\times 10^{-3} \text{ mm}^2/\text{s}$), and ADC_{fast} ($\times 10^{-3} \text{ mm}^2/\text{s}$) in patient 1 with an ischemic stroke. On day 21, f_{fast} and ADC_{fast} are increased when compared with values in normal WM. Normalization of ADC_{slow} is noted on day 21.

TABLE 3: Influence of f_{fast} value on the calculated ADC

f_{fast}	ADC ₁ ($\times 10^{-5}$ mm ² /s)	ADC ₂ ($\times 10^{-5}$ mm ² /s)
0.75	66.42	88.76
0.7	61.19	81.15
0.65	56.31	74.29
0.6	51.76	68.07
0.55	47.50	62.39
0.5	43.51	57.20
0.45	39.75	52.43
0.4	36.21	48.03
0.35	32.87	43.95
0.3	29.72	40.17
0.25	26.73	36.64
0.2	23.89	33.35
0.15	21.20	30.27

Note.—Clinical ADCs (ADC₁ and ADC₂) were calculated on the basis of two b values: 0 and 1000 s/mm². ADC₁ was calculated on the basis of ADC_{slow} and ADC_{fast} in the normal WM of the patients. ADC₂ was calculated on the basis of ADC_{slow} and ADC_{fast} in the ischemic parenchyma of the patients. When f_{fast} is <0.55 both ADC₁ and ADC₂ are decreased.

dence for the assignment of the FDC to the extracellular space.

Proton MR spectroscopy with high- b -value diffusing gradients has been proposed for determining the compartmentation of brain metabolites (19). Evaluation of the compartmentation of brain metabolites in the follow-up of an ischemic stroke might, therefore, be of interest.

References

1. Le Bihan D, Moonen CT, van Zijl PC, et al. **Measuring random microscopic motion of water in tissues with MR imaging: a cat brain study** *J Comput Assist Tomogr* 1991;15:19–25
2. Chien D, Kwong KK, Gress DR, et al. **MR diffusion imaging of cerebral infarction in humans** *AJNR Am J Neuroradiol* 1992; 13: 1097–1102, discussion 1103–1105
3. Moseley ME, Butts K, Yenari MA, et al. **Clinical aspects of DWI** *NMR Biomed* 1995; 8:387–396
4. Warach S, Gaa J, Siewert B, et al. **Acute human stroke studied by whole brain echo planar diffusion-weighted magnetic resonance imaging** *Ann Neurol* 1995;37:231–241
5. Sorensen AG, Wu O, Copen WA, et al. **Human acute cerebral ischemia: detection of changes in water diffusion anisotropy by using MR imaging** *Radiology* 1999;212:785–792
6. Norris DG, Niendorf T, Leibfritz D. **Health and infarcted brain tissues studied at short diffusion times: the origins of apparent restriction and the reduction in apparent diffusion coefficient** *NMR Biomed* 1994;7:304–310
7. Mulkern RV, Zengingonul HP, Robertson RL, et al. **Multi-component apparent diffusion coefficients in human brain: relationship to spin-lattice relaxation** *Magn Reson Med* 2000;44:292–300
8. Niendorf T, Dijkhuizen RM, Norris DG, et al. **Biexponential diffusion attenuation in various states of brain tissue: implications for diffusion-weighted imaging** *Magn Reson Med* 1996;36:847–857
9. Mulkern RV, Vajapeyam S, Robertson RL, et al. **Biexponential apparent diffusion coefficient parametrization in adult vs newborn brain** *Magn Reson Imaging* 2001;19:659–668
10. Mulkern RV, Gudbjartsson H, Westin CF, et al. **Multi-component apparent diffusion coefficients in human brain** *NMR Biomed* 1999; 12:51–62
11. Clark CA, Le Bihan D. **Water diffusion compartmentation and anisotropy at high b values in the human brain** *Magn Reson Med* 2000;44:852–859
12. Inglis BA, Bossart EL, Buckley DL, et al. **Visualization of neural tissue water compartments using biexponential diffusion tensor MRI** *Magn Reson Med* 2001;45:580–587
13. Stejskal EE, Tanner JE. **Spin diffusion measurements: spin echoes in the presence of a time-dependent field gradient** *J Chem Phys* 1965;42:228–292
14. Tofts PS, Lloyd D, Clark CA, et al. **Test liquids for quantitative MRI measurements of self-diffusion coefficient in vivo** *Magn Reson Med* 2000;43:368–374
15. Maier SE, Bogner P, Bajzik G, et al. **Normal brain and brain tumor: multicomponent apparent diffusion coefficient line scan imaging** *Radiology* 2001;219:842–849
16. Nicholson C, Sykova E. **Extracellular space structure revealed by diffusion analysis** *Trends Neurosci* 1998;21:207–215
17. Meyer JR, Gutierrez A, Mock B, et al. **High- b -value diffusion-weighted MR imaging of suspected brain infarction** *AJNR Am J Neuroradiol* 2000;21:1821–1829
18. Duong TQ, Ackerman JJ, Ying HS, Neil JJ. **Evaluation of extra- and intracellular apparent diffusion in normal and globally ischemic rat brain via 19F NMR** *Magn Reson Med* 1998;40:1–13
19. Assaf Y, Cohen Y. **Non-mono-exponential attenuation of water and N-acetyl aspartate signals due to diffusion in brain tissue** *J Magn Reson* 1998;131:69–85